Organic & Biomolecular Chemistry

Dynamic Article Links

Cite this: *Org. Biomol. Chem.*, 2011, **9**, 1092

www.rsc.org/obc

PAPER

Mutation of isoleucine 705 of the oxidosqualene-lanosterol cyclase from *Saccharomyces cerevisiae* affects lanosterol's C/D-ring cyclization and 17α/β-exocyclic side chain stereochemistry†

Tung-Kung Wu,* Yi-Chun Chang, Yuan-Ting Liu, Cheng-Hsiang Chang, Hao-Yu Wen, Wen-Hsuan Li and Wen-Shiang Shie

Received 14th August 2010, Accepted 15th October 2010
DOI: 10.1039/c0ob00582g

Site-saturated substitution in S*accharomyces cerevisiae* oxidosqualene-lanosterol cyclase at Ile705 position produced three chair-boat-chair (C–B–C) truncated tricyclic compounds, two 17α-exocyclic protosteryl intermediates, two protosteryl C-17 truncated rearranged intermediates and the normal biosynthetic product, lanosterol. These results indicated the importance of the Ile705 residue in affecting lanosterol's C/D ring stabilization including 6-6-5 tricyclic and protosteryl C-17 cations and 17α/β–exocyclic side chain stereochemistry.

Introduction

Oxidosqualene cyclases are a mechanistically intriguing family of enzymes that catalyze conversion of a common substrate, acyclic (3*S*)-2,3-oxidosqualene (**1**, **OS**) into diverse and complex tetracyclic or pentacyclic sterols and triterpenoids.[1–6] An intricate and yet highly stereo- and regio-specific cationic cyclization/rearrangement mechanism, that encompasses substrate conformational prefolding, oxirane ring protonation and cleavage, cation/π interaction-directed consecutive tetracyclic ring annulation, 1,2-shifted hydride and methyl groups migration, and final specific deprotonation, has been proposed for the family of enzymes.[7–21] Furthermore, one remarkable phenomenon of oxidosqualene cyclase is that the cyclase-catalyzed reactions can proceed in either an accurate or multifunctional fashion to achieve catalytic perfection or to generate diverse product profiles.[22,23] Many cyclases, including oxidosqualene-lanosterol cyclases (OSCs or ERG7), oxidosqualene-cycloartenol synthases (CASs), β-amyrin synthases (BASs), lupeol synthases (LUP1s), marneral synthase, and cucurbitadienol synthases, make a single product or only minor byproducts (<1% of total); whereas baruol synthase from *Arabidopsis thaliana* is able to make a remarkable number of products.[23–25] In addition, we previously identified several amino acid residues, including Tyr99, Trp232, His234, Phe445, Tyr510, Phe699, and Tyr707 of *Saccharomyces cerevisiae* ERG7, that are critical for enzyme catalysis.[26–34] Site-saturated mutagenesis, which replaces the target residue with each of the other proteinogenic amino acids, of abovementioned residues resulted in the isolation of numerous enzymatic products, including mono-, bi-, tri-, and tetra-cyclic, truncated rearranged or altered deprotonated, as well as carbocationic intermediates traversing the mechanistic barrier from chair-boat-chair (C–B–C) to chair-chair-chair (C–C–C) substrate conformation. Specifically, these residues are all located on the protein's active site cavity surface.

Although amino acids within the protein's active site cavity surface are most likely to contribute to a catalytic outcome, residues outside of the active site can interact with active site residues and subsequently influence the protein structure to promote truncated or altered product formation. An example of a second-tier residue is His477 of *A. thaliana* CAS (CAS^{H477}), which has been demonstrated to form a hydrogen bond with the first-tier residue Tyr410 and is essential to the mechanism of cycloartenol biosynthesis.[35] When CAS^{H477} was mutated to other residues, the disruption of the hydrogen bond to Tyr410 allowed reorientation of the intermediate cation to form other products. To further define other critical amino acid residues involved in catalytic function or enzymatic plasticity, we set up a series of site-directed mutagenesis experiments to investigate the second-tier residues to evaluate the effects on the cyclization/rearrangement mechanism and product specificity/diversity. Among various residues of ERG7 under investigation, Ile705 of *S. cerevisiae* ERG7 (ERG7^{I705}) is further characterized. Ile705 is a highly conserved residue in OSCs and CASs but replaced by Leu in BASs and LUP1s. The ERG7^{I705} is a second-tier residue located proximal to the previously identified first-tier Phe699 and Tyr707 residues.[31,32,34] In addition, mutational study of Leu607 in *Alicyclobacillus acidocaldarius* squalene-hopene cyclase (SHC) (which corresponds to ERG7^{I705}) resulted in formation of abnormal mono- and bi-cyclic truncated products, indicating a functional role during the polycyclization

Department of Biological Science and Technology, National Chiao Tung University, 300, Hsin-Chu, Taiwan (Republic of China). E-mail: tkwmll@mail.nctu.edu.tw

† Electronic supplementary information (ESI) available: NMR spectra of 17α-protosta-20(22),24-dien-3β-ol and protosta-16,24-dien-3β-ol. See DOI: 10.1039/c0ob00582g

Table 1 The product profiles of *S. cerevisiae* ERG7^{I705X} site-saturated and ERG7$^{F699X/I705X}$ double mutants

AA substitution	2	3	4	5	6	7	8	9	10	11
Native	100	—	—	—	—	—	—	—	—	—
I705G	35	23	34	6	—	—	1	1	—	—
I705F	25	—	—	—	21	6	42	6	—	—
I705A	78	13	8	0.3	—	—	—	0.7	—	—
I705V	75	10	15	—	—	—	—	—	—	—
I705D	37	32	30	1	—	—	—	—	—	—
I705N	19	41	37	3	—	—	—	—	—	—
I705Q	25	39	31	5	—	—	—	—	—	—
I705K	12	26.5	53.1	7.6	—	—	—	0.8	—	—
I705T	22	36	41	1	—	—	—	—	—	—
I705C	72	16	11.7	0.3	—	—	—	—	—	—
I705M	88	6	6	—	—	—	—	—	—	—
I705S	12	42	44	1	—	—	—	1	—	—
I705P	81.9	0.1	15	—	—	—	—	3	—	—
I705L	100	—	—	—	—	—	—	—	—	—
Neither cell viability nor product was characterized for the rest of the ERG^{I705X} mutants.										
F699C	No product									
F699C/I705F	No product									
F699T	<0.2	—	—	>99.8	—	—	—	—	—	—
F699T/I705F	36	—	—	45	—	7	12	—	—	—
F699M	1	17	18	46	—	1	—	—	10	7
F699M/I705F	53	17	12	15	—	—	3	—	—	—

process.[13] The ERG7^{I705} might interact with first-tier residues, and subsequently influence the ERG7 active site to achieve a truncated or altered product formation.

Here, we performed the ERG7^{I705X} site-saturated and ERG7$^{F699/I705}$ double mutations using the QuikChange site-directed mutagenesis kit, and transformed the mutated plasmids into a yeast TKW14 strain for genetic selection, as previously described.[29,30] The results showed that the TKW14[pERG7^{I705X}] mutant strains complement ergosterol-independent growth, with the exception of the Tyr (Y), Trp (W), His (H), Glu (E), and Arg (R) substitutions. Subsequently, the product profiles from each mutant were characterized by extracting the non-saponifable lipid (NSL) and applying it onto $AgNO_3$-impregnated silica gel column for separation in order to analyze the product structures by GC-MS and NMR (^{1}H, ^{13}C NMR, DEPT, ^{1}H–^{1}H COSY, HMQC, HMBC, and NOE) spectroscopic techniques.[28–30]

Results and discussion

The product profiles of the ERG7^{I705X} site-saturated mutants with molecular mass of 426 Da are summarized in Table 1. Neither lanosterol (**2**) nor truncated intermediates were isolated from the ERG7$^{I705Y/W/H/E/R}$ non-viable mutants, consistent with the results from genetic analysis. Different viable mutants produced diverse product profiles, ranging from one to five truncated compounds with molecular mass of 426 Da. The ERG7^{I705L} mutants produced lanosterol (**2**) as the sole product. The viable mutants, ERG7$^{I705V/M}$ produced **2** in conjunction with (13α*H*)-isomalabarica-14*E*,17*E*,21-dien-3β-ol (**3**) and (13α*H*)-isomalabarica-14*Z*,17*E*,21-dien-3β-ol (**4**), while ERG7$^{I705D/N/Q/T/C}$ mutants produced **2**, **3**, **4** and protosta-13(17),24-dien-3β-ol (**5**). The ERG7^{I705F} mutant produced **2**, (13α*H*)-isomalabarica-14(26),17*E*,21-trien-3β-ol (**6**), 17α-protosta-20,24-dien-3β-ol (**7**) and two novel yet unidentified compounds with a $C_{30}H_{50}O$ formula. The first of these new compounds was identified by NMR spectroscopy as 17α-protosta-20(22),24-dien-3β-ol (**8**), a product with $\Delta^{20(22),24}$ double bonds and a C-17α exocyclic hydrocarbon side chain configuration, based on following data. The ^{1}H NMR spectra showed three vinyl methyl singlets (δ 1.66, 1.60, 1.52), five methyl singlets (δ 1.11, 0.95, 0.90, 0.80, 0.75) and two olefinic protons (δ 5.07, 5.07). Two tertiary–quaternary substituted double bonds (δ_C 131.85, 124.31 and 137.70, 123.91) were detected by 150 MHz ^{13}C NMR. These results indicated the presence of a tetracyclic nucleus with a terminal hydrocarbon side chain double bond. The HMQC and HMBC spectra showed the following features: (1) the vinyl proton at δ 5.07 (δ_C 123.91, C-22) was coupled to carbons at 13.44 ppm (C-21), 27.77 ppm (C-23) and 51.29 ppm (C-17); (2) the vinyl proton at δ 5.07 (δ_C 131.85, C-24) was coupled to carbons at 18.18 ppm (C-27), 26.16 ppm (C-26) and 124.31 ppm (C-25); (3) the proton at δ 2.65 (δ_C 27.77, C-23) was coupled to carbons at 123.91 ppm (C-22), 124.31 ppm (C-25), 131.85 ppm (C-24) and 137.70 ppm (C-20); (4) the proton at δ 2.07–2.11 (δ_C 51.29, C-17) was coupled to 13.44 ppm (C-21), 25.78 ppm (C-12), 27.77 (C-16), 44.94 (C-13), 123.91 ppm (C-22), and 137.70 ppm (C-20); and (5) the proton at δ 1.59 (δ_C 44.94, C-13) was coupled to carbons at 16.93 ppm (C-30), 23.41 ppm (C-11), 25.78 ppm (C-12), 50.79 ppm (C-14), 137.70 ppm (C-20) and 51.29 ppm (C-17). These correlations established the bond connectivity between the tetracyclic nucleus skeleton and the exocyclic hydrocarbon side chain as well as the $\Delta^{20(22)}$ double bond positions (Fig. 1a). The presence of NOEs among Me-19/Me-29, H-5/Me-18 and H-9/Me-19 confirmed the C–B–C nucleus while Me-30/H-17 and Me-30/H-9, H-3/Me-28 and H-5/Me-28 indicated the C-17α side chain conformation.

The second new compound was characterized as protosta-16,24-dien-3β-ol (**9**), a product with $\Delta^{16,24}$ double bonds based on the following data. The ^{1}H NMR spectra showed two olefinic protons (δ 5.15, 5.09), two vinylic methyl signals (δ 1.65, 1.57) and six methyl singlets (δ 1.17, 0.95, 0.94, 0.93, 0.91, 0.75). The 150 MHz ^{13}C NMR spectrum revealed the presence of two

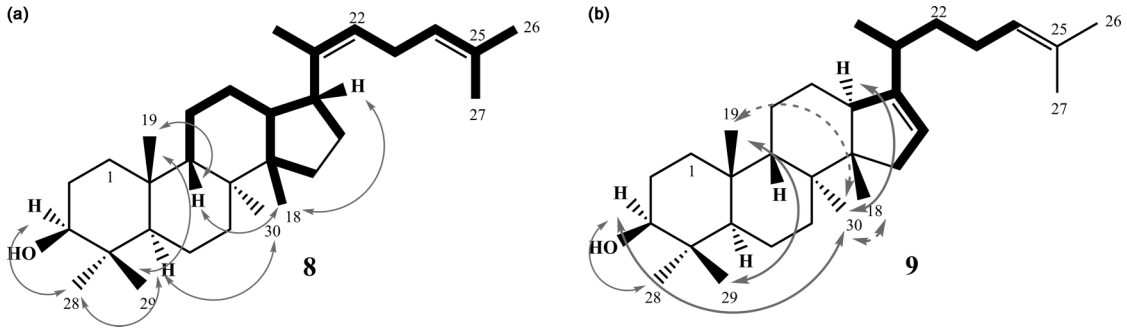

Fig. 1 Bond connectivity and stereochemistry established by HSQC/HMBC (bold bond, ▬) and NOE interaction (curved arrows) of (a) 17α-protosta-20(22),24-dien-3β-ol (**8**) and (b) protosta-16,24-dien-3β-ol (**9**).

tertiary-quaternary substituted double bonds (δ_C 120.48, 151.71 and 125.51, 131.58 ppm). The HMQC and HMBC spectra showed that the methylene protons at δ 1.46–1.49 were attached to the carbon at 35.82 ppm (C-22) and coupled by ^2J to carbons at 34.33 ppm (C-20) and 26.73 ppm (C-23), as well as by ^3J connectivity to carbons at 151.71 ppm (C-17), 125.51 ppm (C-24) and 20.14 (C-21). Furthermore, the C-20 tertiary proton at δ 2.09 showed ^2J and ^3J coupling to C-21, C-22 and C-17, as well as to C-23, C-16 (δ_C 120.48) and C-13 (δ_C 48.77). Finally, the δ 5.15 tertiary vinylic proton attached to the C-16 was coupled by ^2J to C-17 and C-15 (δ_C 39.02), as well as by ^3J connectivity to C-20 and C-13. These correlations established key structural features of the two double bonds located between C-16 and C-17, and between C-24 and C-25. Moreover, the presence of NOEs among H-13/Me-30, Me-30/H-3, H-3/Me-29, Me-28/Me-18 and Me-28/Me-19, as well as the absence of NOEs between Me-19/Me-30 and Me-18/Me-30, confirmed the *trans-syn-trans* stereochemistry and the structure being that of protosta-16,24-dien-3β-ol, a product with $\Delta^{16,24}$ double bonds (Fig. 1b). The ERG7^{I705P} mutant produced **2**, **3**, **4**, and **9** in the ratio of 81.9 : 0.1 : 15 : 3; whereas, the ERG7$^{I705A/K/S}$ mutants produced **2**, **3**, **4**, **5**, and **9** in the ratios of 78 : 13 : 8 : 0.3 : 0.7, 12 : 26 : 53 : 8 : 1 and 12 : 42 : 44 : 1 : 1 respectively. Finally, the ERG7^{I705G} mutant produced **2**, **3**, **4**, **5**, **8**, and **9** in a relative ratio of 35 : 23 : 34 : 6 : 1 : 1. Interestingly, the ERG7^{I705X} mutants produced product profiles similar to that of the ERG7^{F699X} mutants, except for the truncated rearranged protosta-17(20),24-dien-3β-ol (**10**) and C–C tricyclic malabarica-14*E*,17*E*,21-trien-3β-ol (**11**).[34]

The ERG7^{I705X} site-saturated mutants-catalyzed oxidosqualene cyclization/rearrangement pathways (Scheme 1) can be rationalized as follows: For the ERG7^{I705X} viable mutants, **OS** may have entered the enzyme active site cavity with a prefolded C–B–C conformation and cationically cyclizes to a C–B 6-6-5 tricyclic Markonikov C-14 cation (**Ia**) as the first stopping point. Subsequent abstraction of the proton from the C-15 position, with varying predispositions then resulted in the production of **3** and **4**. In the ERG7^{I705F} viable mutant, an alternative abstraction from the C-26 proton produced **6** as the end product. No **OS** can be cyclized to the alternative C–C 6-6-5 tricyclic Markonikov C-14 cation **Ib** by the ERG7^{I705X} mutants. Subsequently, the cation **Ia** can proceed with a C-ring expansion followed by D-ring annulations (**II**) to generate two protosteryl C-20 cations with different stereochemical control at the C-17 position (**IIIa** and **IIIb**). Notably, in the ERG7$^{I705F/G}$ mutants, **IIIa** with a C-17α exocyclic hydrocarbon side chain proceeded the deprotonated termination at C-21 or C-22 position to produce **7** and **8**. Conversely, in most viable mutants, the protosteryl C-20 cation was formed with a C-17β side chain conformation **IIIb**. A backbone rearrangement of H-17α to H-20α, *via* a 1,2 hydride shift, was then able to generate protosteryl C-17 cation **IV**. The ERG7$^{I705F/G/A/K/S/P}$ mutants eliminated a proton from C-16 to generate **9**, while the ERG7$^{I705G/A/D/N//Q/K/T/C/S}$ mutants abstracted the C-13 proton to yield **5**. Finally, subsequent skeletal rearrangements of two methyl-group shifts (Me-14β→Me-13β and Me-8α→Me-14α) and two hydride shifts (H-13α→H17α and H-9β→H8β) generated the lanosteryl C-8/C-9 cation (**V**), which underwent deprotonation at C-9 or C-8 to form **2**, a normal biosynthetic product.

To date, only limited examples for mechanistic transition between C-17α and C-17β have been achieved by use of simple mutations.[33,36] We previously isolated 17α-protosta-20,24-dien-3β-ol (**7**) from the ERG7^{F699M} muant, suggesting the mutational effect on generation of protosteryl C-20 cation with C-17α stereochemical control (**IIIa**) and subsequent deprotonation at C-21 to form **7**. In the present study, the ERG7^{I705F} and ERG7^{I705G} muants were able to generate the **IIIa** cation, proceded by deprotonated termination at the C-22 position to yield 17α-protosta-20(22),24-dien-3β-ol (**8**). These observations provided further support for the mechanism of plasticity of the active site residues and the notion that the replacement of a single amino acid residue can dramatically affect catalytic fidelity. It is conceivable that the isolation of truncated rearranged intermediates **9**, but not **5**, from the ERG7$^{I705F/P}$ mutant indicated that the Phe or Pro substitution also was able to determine the normal protosteryl C-20 cation with C-17β stereochemistry and control the proton abstraction from C-16 position, as opposed to the C-13 position. Nevertheless, most of the viable substitutions at the Ile705 position affected tricyclic cation **Ia** and protosteryl C-17 cation **IV**, resulting in the production of **3**, **4** and **5** as truncated products.

The similarity of product profiles produced by both ERG7^{I705F} and ERG7^{F699X} mutants provoked us to investigate the amino acid interactions between first- and second-tier residues in the product profile. The ERG7^{F699C}, ERG7^{F699T}, and ERG7^{F699M} mutated plasmids, which produced either no, single, or diverse product profiles, were further subjected to a second Ile705Phe (I705F) mutation (Table 1). As expected, the ERG7$^{F699C/I705F}$ double mutant caused yeast non-viability and no product formation, supporting the importance of F699C mutational effect on the regulation of enzyme activity. Alternatively, the ERG7$^{F699T/I705F}$ double mutant altered product specificity from a single compound **5** (>99.8%) to diverse products **2**, **5**, **7**, and **8** in the relative ratio of 36 : 45 : 7 : 12.

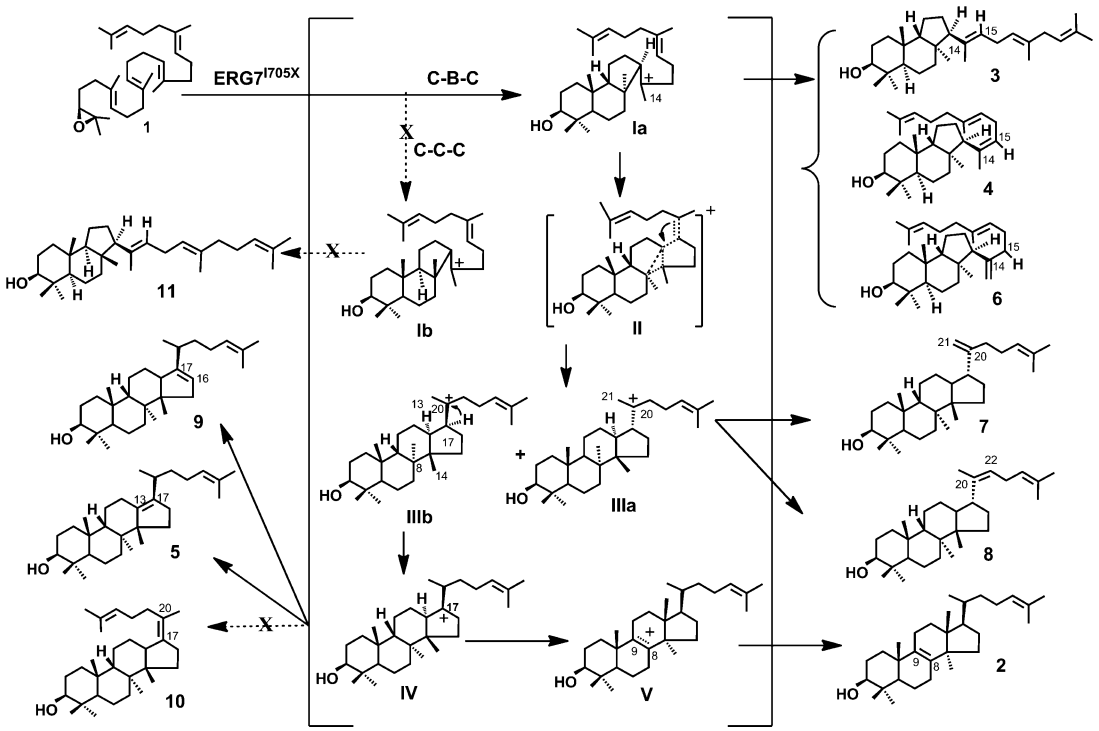

Scheme 1 The proposed cyclization/rearrangement pathways of oxidosqualene within *S. cerevisiae* ERG7^{I705X} mutants.

This finding indicated that the electrostatic interactions between Ile705 and Phe699 play a role in product specificity. Finally, the ERG7$^{F699M/I705F}$ double mutant changed product profile from **2**, **6**, **7**, **8** and **9** to **2**, **3**, **4**, **5** and **8**, a product profile shift from that of ERG7^{I705F} single mutant towards that of ERG7^{F699M} or ERG7^{Y99X} single mutant. This shift revealed a functional role for the Ile705 to Phe substitution in influencing the Phe699 or Tyr99 residues and the consequent regulation of the substrate's exocyclic hydrocarbon side chain stereochemistry.[32–34]

The homology structural model of ERG7 complexed with cation **IV** was determined by using the human OSC crystal structure as template. The structural analysis indicated that the Ile705 is a second-tier residue and spatially proximal to the first-tier residues Tyr99 and Phe699 (Fig. 2).[20,21] Our previous ERG7^{F699X} site-saturated mutagenesis results had indicated that Phe699, in conjunction with Tyr99, His234, and Tyr707, may play a functional role in restricting the C–B–C conformation and/or side chain rotation, as well as in stabilizing the protosteryl C-17 cation.[26–34] Perhaps, the ERG7^{I705} is able to interact with the first-tier residues and subsequently influence the ERG7 active site to promote truncated or altered product formation. Substitution of Ile705 with Phe may disrupt the stabilization of Phe699 to protosteryl C-17 cation or Tyr99 to C–B 6-6-5 tricyclic Markovnikov C-14 cation.[33,34] This, in turn, could have impaired the catalytic fidelity of the enzyme and resulted in the shift of the product profiles towards that of ERG7^{F699M} and ERG7^{Y99X}.[33,34]

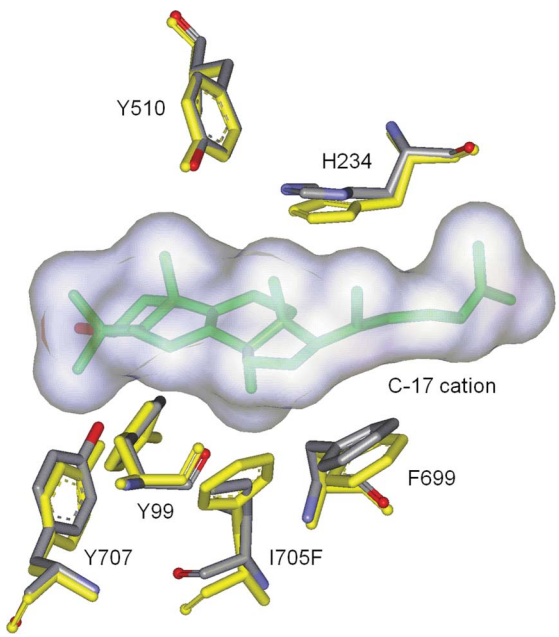

Fig. 2 The superimposed homology model of *S. cerevisiae* ERG7^{I705X} complexed with protosteryl C-17 cation.

Conclusions

In summary, our ERG7^{I705X} site-saturated and ERG7$^{F699X/I705F}$ double mutation experiments were able to unravel the catalytic role of the second-tier Ile705 residue. Specifically, our findings indicated functional roles for Ile705 in mediating the C–B tricyclic Markovnikov C-14 cation, 17α/17β stereochemistry of exocyclic hydrocarbon side chain and protosteryl C-17 cation for final deprotonation product formation. Moreover, a product with tailored specificity could be obtained *via* subtle molecular interaction changes between the second-tier residue and its neighboring first-tier amino acids.

Experimental

Generation and analysis of mutant extracts. Mutagenesis of Ile705 in the *S. cerevisiae* ERG7 wild-type gene was performed using the QuikChange site-directed mutagenesis kit (Stratagene, La Jolla, CA). The degenerate site-saturated mutagenic primers for Ile705 were the following, with substitutions underlined and silent mutation italicized:

ERG7I705X1:
5'-d(CACTCTTGTGCANNNGAATACCCGAGTT*ATCGAT*TC)-3'

ERG7SQCYT2:
5'-d(GA*ATCGAT*AACTCGGGTATTCNNNTGCACAAGAGTG)-3

The PCR reaction mix was composed of 0.8 mM of dNTPs, 100 ng of pRS314ERG7WT plasmid template, 1X Pfu polymerase buffer, 1 μL of each primer, 2.5 U of Pfu DNA polymerase and ddH2O to a final volume of 20 μL. The reaction mixture was denatured at 95 °C for two min, and then run for 18 cycles of denaturation at 95 °C for 30 s, annealing at 50 °C for one min, polymerization at 68 °C for one min; a final extension was carried out at 68 °C for 16 min. The PCR products were incubated with Dpn I at 37 °C for three hours to digest the parental supercoiled DNA. The digested PCR products were mixed with 100 μL of *E. coli* XL-Blue competent cells and incubated on ice for 20 min. The cells were transformed by the heat shock method for one min at 42 °C followed by one min on ice. The cells were immediately transferred to 1 mL Luria–Bertani (LB) medium and shaken at 200 rpm for one hour at 37 °C. Then, the cells were centrifuged at 6,000 × g for one min and propagated on an LB plate containing 100 μg mL^{-1} ampicillin incubated at 37 °C for 16 h. The resulting colonies were individually picked and cultured overnight at 37 °C in 3 mL of LB medium containing 100 μg mL^{-1} ampicillin. The plasmid DNAs were isolated by plasmid miniprep purification kit, according to the manufacturer's instruction.

The mutations were confirmed by DNA sequencing and subsequently electroporated into the yeast strain TKW14 and selected for growth on SD+Ade+Lys+His+Met+Ura+hemin +G418+Erg plates. The plasmids were then selected on SD+Ade+Lys+His+Met+Ura+hemin+G418+5-FOA plates for complementation of cyclase activity as described previously. Transformants were grown in SD+ Ade+Lys+His+Met+Ura +hemin+G418+Erg medium for non-saponifiable lipid (NSL) extraction and column chromatography. Products were acetylated, separated using $AgNO_3$-impregnated silica gel column chromatography, and characterized by GC-MS and NMR (^{1}H, ^{13}C NMR, DEPT, HSQC, HMBC, and NOE) spectroscopic techniques.

Chemical shifts of 17α-protosta-20(22),24-dien-3β-ol (8). Chemical shifts were referenced to $Si(CH_3)_4$ and are generally accurate to +0.01 ppm. ^{1}H NMR (600 MHz, CD_2Cl_2): δ 5.07 (t, 2H, 1H for H-22, 1H for H-24), 3.186 (dd, J = 15, 5 Hz, 1H, H-3α), 2.653 (t, J = 7.05 Hz, 1H, H-23) 1.011–2.064 (m,1H, H-17), 1.926–1.965 (m, 1H, H-7), 1.774–1.707 (m, 1H, H-16), 1.663 (d, 1H, Me-26), 1.66–1.63 (m, 1H, H-2), 1.603 (s, 1H, Me-27), 1.60–1.55 (m, 2H, 1H for H-13, 1H for H-2), 1.60 (s, 3H, H-27), 1.52 (s, 3H, Me-21), 1.54–1.51 (m, 1H, H-6), 1.51–1.47 (m, 1H, H-6), 1.51–1.45 (m, 2H, 1H for H-9, 1H for H-15), 1.47–1.41 (m, 3H, 1H for H-12, 1H for H-11, 1H for H5), 1.42–1.38 (m, 3H, 2H for H-1, 1H for H-16), 1.222–1.20 (m, 1H, H-11), 1.20–1.18 (m, 2H, 1H for H-7, 1H for H–H-6), 1.055 (s, 3H, Me-30), 0.949 (s, 3H, Me-19), 0.799 (s, 3H, Me-18), 0.751(s, 3H, Me-29). 1.734–1.714 (dddd, 1H, H-12), 1.651 (s, 3H Me-26), 1.659–1.584 (m, 4*H*,2H for H-2, 1H for H-15, 1H for H-9), 1.566 (s, 3H, H-27), 1.574–1.532 (m, 4H, 1H for H-5, 1H for H-6, 2H for H-11), 1.494–1.457 (m, 1H, H-22), 1.408–1.388 (m, 2H, H-1),1.408–1.234 (m, 1H, H-12), 1.260–1.211 (m, 1H, H-6), 1.225–1.158 (m, 2*H*,1H for H-22, 1H for H-7), 1.172 (s, 3H, Me-30), 0.952 (s, 3H, Me-29), 0.940 (s, 3H, Me-21), 0.930 (s, 3H, Me-18), 0.909 (s, 3H, Me-19), 0.752 (s, 3H, Me-28). ^{13}C NMR Spectra δ 33.87 (C-1), 30.02 (C-2), 79.85 (C-3), 39.94 (C-4), 48.72 (C-5), 19.27 (C-6), 35.89 (C-7), 40.37 (C-8), 46.72 (C-9), 37.66 (C-10), 23.41 (C-11), 25.78 (C-12), 44.94(C-13), 50.79 (C-14), 32.33 (C-15), 27.77 (C-16), 51.27 (C-17), 16.93 (C-18), 23.2 (C-19), 137.7 (C-20), 13.44 (C-21), 123.91 (C-22), 27.77 (C-23), 131.85 (C-24), 124.31 (C-25), 26.16 (C-26), 18.18 (C-27), 16.71 (C-28), 29.61 (C-29), 22.27 (C-30).

Chemical shifts of protosta-16,24-dien-3β-ol (9). Chemical shifts were referenced to $Si(CH_3)_4$ and are generally accurate to +0.01 ppm. ^{1}H NMR (600 MHz, CD_2Cl_2): δ 5.15 (septet, 1H, H-15), 5.087 (tt, J = 5.8 Hz, 1H, H-3α), 3.194 (dd, J = 11.7, 5.1 Hz, 1H, H-3α), 3.194 (dd, J = 11.7, 5.1 Hz, 1H, H-3α), 2.638 (dd, J = 12.9, 3.2 Hz, 1H, H-13) 2.219 (d, J = 14.652 Hz,1H, H-15), 2.092 (dd, J = 14.115, 6.77 Hz, 1H, H-20), 1948–1.909 (m, 2H, H-23), 1.900–1.879 (m, 1H, H-7), 1.734–1.714 (dddd, 1H, H-12), 1.651 (s, 3H Me-26), 1.659–1.584 (m, 4*H*,2H for H-2, 1H for H-15, 1H for H-9), 1.566 (s, 3H, H-27), 1.574–1.532 (m, 4H, 1H for H-5, 1H for H-6, 2H for H-11), 1.494–1.457 (m, 1H, H-22), 1.408–1.388 (m, 2H, H-1),1.408–1.234 (m, 1H, H-12), 1.260–1.211 (m, 1H, H-6), 1.225–1.158 (m, 2*H*,1H for H-22, 1H for H-7), 1.172 (s, 3H, Me-30), 0.952 (s, 3H, Me-29), 0.940 (s, 3H, Me-21), 0.930 (s, 3H, Me-18), 0.909 (s, 3H, Me-19), 0.752 (s, 3H, Me-28). ^{13}C NMR Spectra δ 33.47 (C-1), 29.86 (C-2), 79.73 (C-3), 39.79 (C-4), 47.99 (C-5), 18.75 (C-6), 34.72 (C-7), 39.53 (C-8), 46.32 (C-9), 37.55 (C-10), 23.77 (C-11), 24.12 (C-12), 48.77(C-13), 54.00 (C-14), 39.02 (C-15), 120.48 (C-16), 151.71 (C-17), 24.29 (C-18), 22.75 (C-19), 34.33 (C-20), 20.14 (C-21), 35.82 (C-22), 26.73 (C-23), 125.51 (C-24), 131.58 (C-25), 26.00 (C-26), 17.93 (C-27), 16.49 (C-28), 29.48 (C-29), 24.29 (C-30).

Acknowledgements

We are grateful to Dr John H. Griffin and Prof. Tahsin J. Chow for helpful advice. We thank the MOE ATU Plan, the National Chiao Tung University as well as the National Science Council of the Republic of China for financial support of this research under Contract No. NSC-98-2627-M-009-007, and NSC-98-2627-M-009-008.

Notes and references

1 I. Abe, M. Rohmer and G. D. Prestwich, *Chem. Rev.*, 1993, **93**, 2189–2206.
2 K. U. Wendt, G. E. Schulz, E. J. Corey and D. R. Liu, *Angew. Chem. Int. Ed.*, 2000, **39**, 2812–2833.
3 R. Xu, G. C. Fazio and S. P. T. Matsuda, *Phytochemistry*, 2004, **65**, 261–291.
4 I. Abe, *Nat. Prod. Rep.*, 2007, **24**, 1311–1331.
5 T. K. Wu and J. H. Griffin, *Biochemistry*, 2002, **41**, 8238–8244.
6 T. K. Wu, C. H. Chang, Y. T. Liu and T. T. Wang, *Chem. Rec.*, 2008, **8**, 302–325.
7 I. Abe, *Nat. Prod. Rep.*, 2007, **24**, 1311–1331.

8 R. Kelly, S. M. Miller, M. H. Lai and D. R. Kirsch, *Gene*, 1990, **87**, 177–183.
9 C. J. Buntel and J. H. Griffin, *J. Am. Chem. Soc.*, 1992, **114**, 9711–9713.
10 Z. Shi, C. J. Buntel and J. H. Griffin, *Proc. Natl. Acad. Sci. U. S. A.*, 1994, **91**, 7370–7374.
11 T. Kushiro, M. Shibuya and Y. Ebizuka, *Eur. J. Biochem.*, 1998, **256**, 238–244.
12 T. Husselstein-Muller, H. Schaller and P. Benveniste, *Plant Mol. Biol.*, 2001, **45**, 75–92.
13 T. Hoshino and T. Sato, *Chem. Commun.*, 2002, 291–301.
14 I. Iturbe-Ormaetxe, K. Haralampidis, K. papadopoulou and A. E. Osbourn, *Plant Mol. Biol.*, 2003, **51**, 731–743.
15 T. Merkofer, C. Pale-Grosdemange, M. Rohmer and K. Poralla, *Tetrahedron Lett.*, 1999, **40**, 2121–2124.
16 E. J. Corey, S. P. Matsuda and B. Bartel, *Proc. Natl. Acad. Sci. U. S. A.*, 1993, **90**, 11628–11632.
17 E. J. Corey, S. P. T. Matsuda and B. Bartel, *Proc. Natl. Acad. Sci. U. S. A.*, 1994, **91**, 2211–2215.
18 C. H. Baker, S. P. T. Matsuda, D. R. Liu and E. J. Corey, *Biochem. Biophys. Res. Commun.*, 1995, **213**, 154–160.
19 J. B. Herrera, B. Bartel, W. K. Wilson and S. P. Matsuda, *Phytochemistry*, 1998, **49**, 1905–1911.
20 R. Thoma, T. Schulz-Gasch, B. D'Arcy, J. Benz, J. Aebi, H. Dehmlow, M. Hennig, M. Stihle and A. Ruf, *Nature*, 2004, **432**, 118–122.
21 K. U. Wendt, *Angew. Chem., Int. Ed.*, 2005, **44**, 3966–3971.
22 D. R. Phillips, J. M. Rasbery, B. Bartel and S. P. Matsuda, *Curr. Opin. Plant Biol.*, 2006, **9**, 305–314.
23 S. Lodeiro, Q. Xiong, W. K. Wilson, M. D. Kolesnikova, C. S. Onak and S. P. Matsuda, *J. Am. Chem. Soc.*, 2007, **129**, 11213–11222.
24 J. B. Herrera, W. K. Wilson and S. P. T. Matsuda, *J. Am. Chem. Soc.*, 2000, **122**, 6765–6766.
25 S. Lodeiro, M. J. Segura, M. Stahl, T. Schulz-Gasch and S. P. T. Matsuda, *ChemBioChem*, 2004, **5**, 1581–1585.
26 T. K. Wu and C. H. Chang, *ChemBioChem*, 2004, **5**, 1712–1715.
27 T. K. Wu, Y. T. Liu and C. H. Chang, *ChemBioChem*, 2005, **6**, 1177–1181.
28 T. K. Wu, M. T. Yu, Y. T. Liu, C. H. Chang, H. J. Wang and E. W. G. Diau, *Org. Lett.*, 2006, **8**, 1319–1322.
29 T. K. Wu, Y. T. Liu, C. H. Chang, M. T. Yu and H. J. Wang, *J. Am. Chem. Soc.*, 2006, **128**, 6414–6419.
30 T. K. Wu, Y. T. Liu, F. H. Chiu and C. H. Chang, *Org. Lett.*, 2006, **8**, 4691–4694.
31 T. K. Wu, H. Y. Wen, C. H. Chang and Y. T. Liu, *Org. Lett.*, 2008, **10**, 2529–2532.
32 T. K. Wu, T. T. Wang, C. H. Chang and Y. T. Liu, *Org. Lett.*, 2008, **10**, 4959–4962.
33 T. K. Wu, W. H. Li, C. H. Chang, H. Y. Wen, Y. T. Liu and Y. C. Chang, *Eur. J. Org. Chem.*, 2009, 5731–5737.
34 T. K. Wu, C. H. Chang, H. Y. Wen, Y. T. Liu, W. H. Li, T. T. Wang and W. S. Shie, *Org. Lett.*, 2010, **12**, 500–503.
35 M. J. R. Segura, S. Lodeiro, M. M. Meyer, A. J. Patel and S. P. T. Matsuda, *Org. Lett.*, 2002, **4**, 4459–4462.
36 T. Hoshino, T. Abe and M. Kouda, *Chem. Commun.*, 2000, 441–442.